Water Supply

Water Supply Vol 22 No 1, 686 doi: 10.2166/ws.2021.241

Hydrochemical characteristics and groundwater quality appraisal for irrigation uses in the Lan-gan region, Northern Anhui Province, East China

Jie Ma[a,b,*], Song Chen[a,b], Diandian Ding[a,b] and Jingyu Zhao[a,b]

[a] School of Resources and Civil Engineering, Suzhou University, Suzhou, Anhui, China

[b] Key Laboratory of Mine Water Resource Utilization of Anhui Higher Education Institutes, Suzhou University, Suzhou, Anhui, China

*Corresponding author. E-mail: ahszumajie@163.com

JM, 0000-0002-7693-6038

ABSTRACT

Lan-gan region, one of traditional agricultural production base in northern Anhui Province, East China, has rare hydrochemical reports on the formation mechanism and irrigation assessment of the Quaternary deeper confined groundwater aquifer. To better master hydrochemical characteristics, solute source, and irrigation properties, twenty-five water samples were collected from individual wells. The Gibbs diagram, Piper diagram, ionic ratio, and multivariate statistical analysis were carried out to delineate the hydrochemical facies and water–rock interactions. Meanwhile, USSL and Wilcox diagrams, and irrigation water quality indices were conducted to illustrate the suitability for irrigation. The results indicate that cations and anions are in the order of $Ca^{2+} > Na^{+} > Mg^{2+} > K^{+}$ and $HCO_3^- > SO_4^{2-} > Cl^-$, respectively. Ca-$HCO_3$ is the main hydrochemical type. Water–rock interactions include silicate weathering, carbonate dissolution, halite dissolution and sulfate dissolution. Based on electrical conductivity (EC) value, the majority of the samples are permissible for irrigation, whereas only 12% of the samples were found good for irrigation. The risidual sodium carbonate (RSC), sodium adsorption ratio (SAR), and percentage sodium (%Na), combined with Wilcox and USSL diagrams, demonstrate that the groundwater samples are permissible for irrigation purposes.

Key words: irrigation assessment, multivariate statistical analysis, solute source, water–rock interactions

HIGHLIGHTS

- The study provides additional information about the hydrogeological information of the study area.
- Detailed hydrochemical graphical methods delineate the hydrochemical facies and water–rock interactions.
- Ionic ratio and multivariate statistical analysis were carried out to delineate the hydrochemical characteristics and solute origin.
- Irrigation water quality is evaluated for irrigation purposes.

INTRODUCTION

Water is an excellent natural resource on earth. During the processes of precipitation, runoff, seepage as well as anthropogenic activities, the extent and degree of water–rock interactions changes the hydrochemical components (Li *et al.* 2018). Hydrochemical information abstracted from the interactions can be applied to reveal hydrochemical characteristics, processes and mechanisms, the sources of the major ions, pollution source, and the suitability for irrigation, etc (Alemayehu *et al.* 2020; Yidana *et al.* 2020).

Surface water is vulnerable and scarce in many areas, so groundwater plays a significant role for economic development and human survival, and it has acted as a major source for drinking and irrigation. In order to utilize and protect groundwater efficiently, it is necessary to grasp a series of physicochemical parameters such as electrical conductivity (EC), total dissolved solids (TDS), and major ions (Ghalib 2017). To get an insight into water–rock interactions and hydrochemical characteristics, conventional hydrochemical methods and multivariate statistical methods have been used to investigate various water bodies (Xiao *et al.* 2015; Pazand *et al.* 2018; Kshetrimayum & Laishram 2020). The suitability of irrigation has been reported and numerous studies have been implemented to evaluate irrigation (Sharma *et al.* 2017; Adimalla 2020; Ghazaryan *et al.* 2020). In China, a rural revitalization strategy and the construction of well-facilitated farmland have been proposed to protect human health, optimize land use structure and layout, and encourage the strengthening of the ecological environment, etc. The sustainable development of irrigated agriculture and high quality groundwater are the effective guarantee for realizing the above-mentioned goals.

In and around the study region, owing to the abundant mineral resources, coal, coalbed methane, and refractory clay have been mined for several decades. Many studies have focused on the rivers, collapse ponds and water-inrush aquifers of coal-mines with respect to hydrochemical composition and water quality assessment (Sun & Gui 2015; Ma *et al.* 2017; Qian *et al.* 2018; Zhang *et al.* 2020). A detailed study on the hydrochemical characteristics, evolution of solute components, and safety evaluation for irrigation purposes of groundwater has rarely been reported in such a traditional agricultural production base. Therefore, a more systematic investigation and irrigation appraisal in a traditional agricultural production base were carried out with the objective of analyzing the relationship between the major ions, depicting the hydrochemical characteristics, and evaluating the irrigation water quality of the groundwater in Lan-gan region, Northern Anhui Province, East China. The results will be helpful in protecting the groundwater quality, and supporting the sustainable development and management of the groundwater resource in the Lan-gan region.

STUDY AREA

The Lan-gan region, which is famous for its traditional agriculture, is situated in northern Anhui Province, East China. The region is located at 33°55′00″-33°56′00″ latitude and 117°16′00″-117°18′00″ longitude with a total area of 147 Km^2 (Figure 1). The east and west of the study area is comprised of hills and plains, respectively.

The most important economic pillar of the area is agriculture. Local farmers mainly cultivate corn and soybean grown from June to October, and wheat raised from October to June of the next year. Meanwhile, watermelon, peach, peanut, cotton, sesame, rape, sweet potato, and other economic crops are also planted. During the period of applying fertilizer, the amount of urea and compound fertilizer used depends on the type of crops. In addition, breeding of chicken, duck, pig and sheep constitutes additional income for farmers.

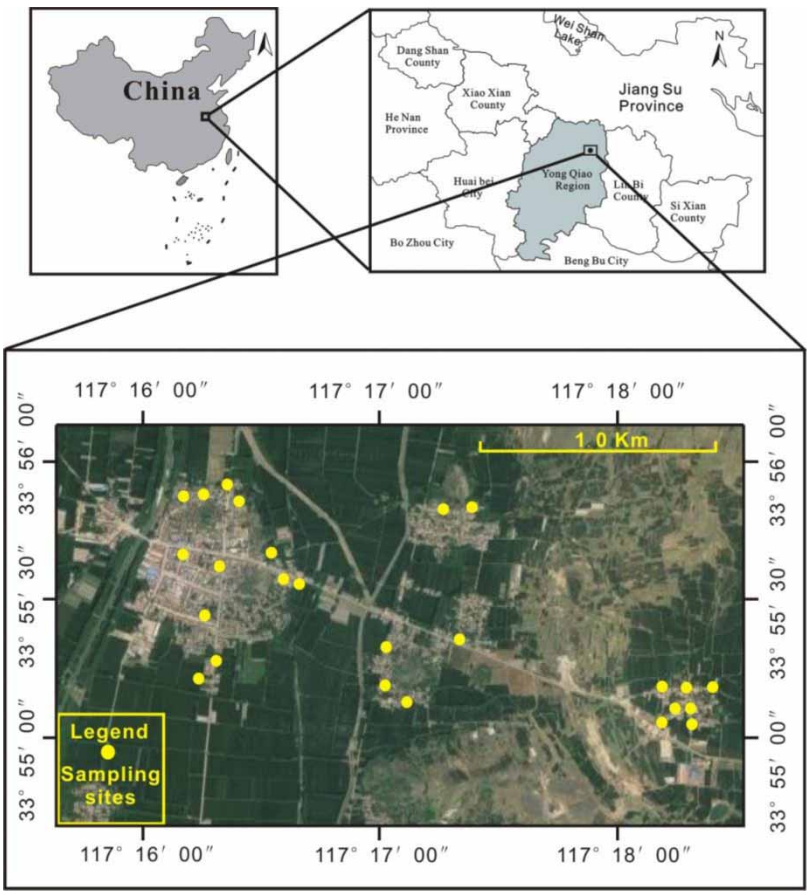

Figure 1 | Groundwater sampling location of the study area.

The study region experiences a temperate humid climate with dry-cold winter and rainy summer. The mean annual air temperature is 14.4 °C, and the hottest month is July with an average temperature of 27.4 °C, and the coldest month is January with an average temperature of 0 °C. The average annual rainfall and evaporation is around 857 mm and 1,060 mm, respectively. The rainfall is concentrated between July and August.

Geologically, the formation of the study area consists of Quaternary and Neopoterozoic Qingbaikouan systems. According to a regional survey and drilling verification, from the bottom to top, the formations are Shijia group of the Qingbaikouan system, Wangshan group of Qingbaikouan system, and Quaternary system, respectively. The Shijia group is about 402 m thick, and outcrops in the form of hills. The lower Shijia group is formed by shale and a shaly sand interbed, whilst the upper Shijia group is mainly composed of shale interbedded with silty sandstone. The Wangshan group is subdivided into three sequences: (1) the lower Wangshan group constitutes dolomitic limestone and marl with a thickness of 96.9 m; (2) the middle Wangshan group is characterized by dolomitic limestone and limestone, with average thickness of about 182.4 m; (3) the upper Wangshan group consists of limestone and dolomitic limestone with an average thickness of 94 m. The Quaternary system comprises sand, clay and silty clay. The thickness of the formation is approximately 80–140 m.

Hydrogeologically, based on the strata's lithology and void development, two Quaternary loose aquifers have been recognized: a shallow unconfined pore aquifer and a deeper confined pore aquifer contacted with a weathered carbonated crust. At first, local inhabitants extracted groundwater from the shallow pore aquifer for their livelihoods but, with the deterioration of water quality and decrease of water yield, local residents now exploit the deeper confined pore aquifer. In this study, we focus on the deeper confined pore aquifer, with a sampling depth from 35 m to 85 m, depicting its hydrochemical characteristics and evolution processes, and assessing its suitability for irrigation purposes.

MATERIALS AND METHODS

Before the sampling campaign, a regional investigation and interviews with local residents were carried out to grasp the fundamental geological and hydrogeological conditions, and the development and usage status of the groundwater. The groundwater was usually abstracted from individual dug wells with a depth varying from 35 m to 105 m. Sampling wells were selected from those still in use. The selection of groundwater sampling sites is combined with the location of residential wells, and the selection principle should meet the specification requirements as far as possible; meanwhile, the groundwater sampling sites selected reflect regional groundwater hydrochemical characteristics. Based on the above sampling considerations, 25 groundwater samples were collected during October, 2020 (Figure 1). Before sampling, the bottles were rinsed 3–5 times with the groundwater to be sampled. During the sampling, the EC, pH, and TDS were measured *in situ* after pumping the water for 5–10 minutes. Apart from sampling, imperative original information including the depth of the well, and lithology of the pumping stratum were also recorded. The samples were transported to the National Engineering Research Center of Coal Mine Water Hazard Controlling, China. The filtration and HCO_3^- titration tests were completed on the same day. Major cations (Na^+, K^+, Ca^{2+}, and Mg^{2+}) and anions (SO_4^{2-} and Cl^-) were analyzed by DIONEX-600 and 900 ion chromatography, respectively. Ionic balance errors were calculated within $\pm 10\%$.

Descriptive statistics including minimum, maximum, mean, and coefficient of variation were analyzed by Mystat 12 software. The Gibbs diagram and Durov diagram were conducted to explain the formation mechanism controlling groundwater hydrochemistry. Ionic ratios, correlation analysis, and principal component analysis were implemented using SPSS 16 to delineate the water–rock interactions and solute source of the groundwater. The EC, sodium adsorption ratio (SAR), percentage sodium (%Na), as well as USSL and Wilcox diagrams were used to evaluate the suitability for irrigation purposes.

RESULTS AND DISCUSSION

General hydrochemistry

In order to grasp the variation of hydrochemical features of the groundwater, a statistical summary of physicochemical parameters is shown in Table 1. The EC values range from 645.00 μS/cm to 1,912.00 μS/cm with a mean value of 1,151.44 μS/cm. The pH values vary from 6.96 to 7.96 with an average value of 7.46, indicating that the samples are neutral to slightly alkaline over the study area. The values of TDS range between 292.00 mg/L and 1,253.00 mg/L with a mean of 569.64 mg/L implying that most of the samples are classified as freshwater.

Cations and anions constitute the principle hydrochemical components of the groundwater. The concentrations of Na^+, K^+, Mg^{2+}, and Ca^{2+} are observed in the range of 7.00–198.08, 0.00–20.94, 11.53–101.42, and 102.91–332.38 mg/L, respectively.

Table 1 | Statistics of physico-chemical parameters of the groundwater samples

Indices	Min	Max	Mean	C. V.[a]
Na^+	7.00	198.08	47.75	45.79
K^+	0.00	20.94	2.53	4.83
Mg^{2+}	11.53	101.42	38.48	24.27
Ca^{2+}	102.91	332.38	164.80	56.26
Cl^-	14.80	254.49	78.07	62.85
SO_4^{2-}	21.67	363.56	97.19	83.76
HCO_3^-	261.56	837.32	476.91	122.74
pH	6.96	7.96	7.46	0.29
EC	645.00	1,912.00	1,151.44	361.44
TDS	292.00	1,253.00	569.64	235.34

Except pH (no unit) and EC (in μS/cm), all the other parameters are in mg/L.
[a]C. V., Coefficient of variation.

The concentration of Cl^-, SO_4^{2-}, and HCO_3^- are within the range of 14.80–254.49, 21.67–363.56, and 261.56–837.32 mg/L, respectively. The order based on the average concentration is $Ca^{2+} > Na^+ > Mg^{2+} > K^+$ and $HCO_3^- > SO_4^{2-} > Cl^-$ for cations and anions, respectively. It is obvious that Ca^{2+} and HCO_3^- are the most abundant cations and anions in the groundwater.

Durov diagrams have been widely used to delineate hydrochemical characteristics (Alemayehu *et al.* 2020; Kshetrimayum & Laishram 2020). Figure 2 reveals that the groundwater samples are dominated by alkali-earth metal cations (Ca^{2+} and Mg^{2+}) and bicarbonate anions with most TDS concentrations less than 1,000 mg/L, indicating that the Ca-HCO_3 type is the main hydrochemical type.

This hydrochemical type can be confirmed by the stratigraphic lithology and runoff condition. The groundwater samples were collected from bedrock surface consisting of carbonate rock such as dolomitic limestone, limy dolomite, dolomite and limestone. Meanwhile, the local topography is mainly composed of hill and plains with short runoff path. As rainwater and surface water percolates through the soil, it reacts with carbon dioxide engendering carbonic acid and the composition of the stratum flowing through, inducing dissolution during contact processes. So, according to its lithology and short runoff path,

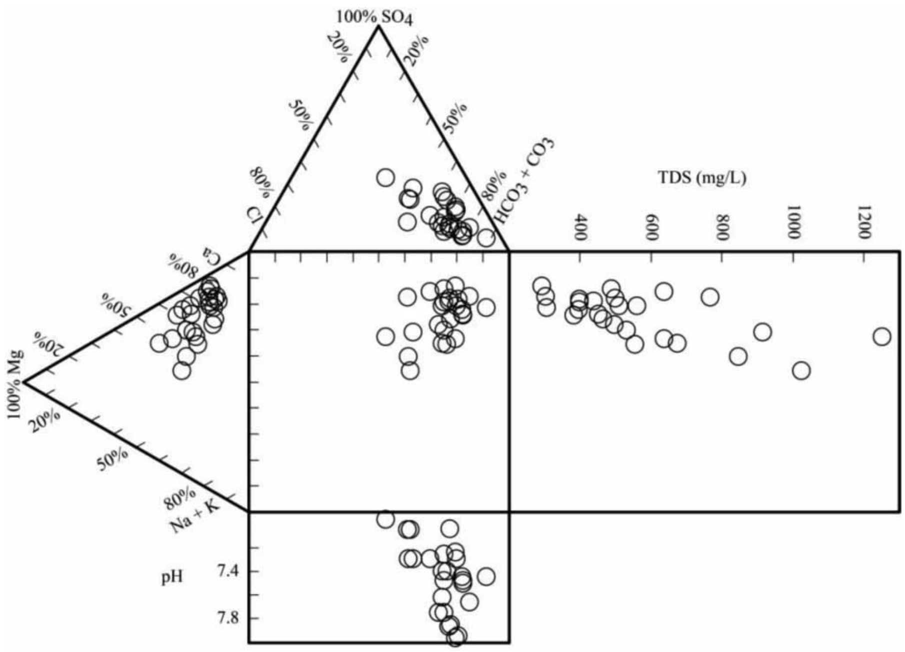

Figure 2 | Durov Diagram of the groundwater samples.

the Ca-HCO_3 type is the most important hydrochemical type in the study area, which is consistent with the sequence of HCO_3^- (recharge area)→ SO_4^{2-} (run off area) → Cl^- (discharge area) along the groundwater flow for the anions.

Mechanism controlling groundwater hydrochemistry

Gibbs proposed three end members to highlight the controlling hydrochemical factors on element composition, including evaporation dominance, rock dominance, and precipitation dominance (Li *et al.* 2018; Adimalla 2020). The concentration ratios of $Cl^-/(Cl^- + HCO_3^-)$ and $(Na^+)/(Na^+ + Ca^{2+})$ as a function of TDS were plotted in Gibbs diagram to illustrate the relationship between hydrochemical components of the aquifer matrix. As shown in Figure 3, the samples were characterized by a relative concentration of TDS and a wide range of $Cl^-/(Cl^- + HCO_3^-)$ and $(Na^+)/(Na^+ + Ca^{2+})$, indicating that water–rock interactions act as a vital role in influencing the hydrochemistry.

According to the molar ratio of Ca^{2+}/Na^+, HCO_3^-/Na^+, and Mg^{2+}/Na^+, three dominant interactions between groundwater and rocks can be distinguished, which are evaporation dissolution, carbonate dissolution and silicate weathering, respectively (Xiao *et al.* 2015; Olea-Olea *et al.* 2020). As can be seen from Figure 4, the ratio of Ca^{2+}/Na^+, HCO_3^-/Na^+ and Mg^{2+}/Na^+ range from 2.61 to 34.90, 1.59 to 7.71 and 1.59 to 14.09, respectively. Most of the samples were plotted in the area of carbonate dissolution and silicate weathering, which further suggests that the hydrochemical characteristics of the groundwater samples are influenced by water–rock interactions. These two hydrochemical water–rock interactions contribute sodium, calcium, magnesium, and bicarbonate to the groundwater components.

Source of solute components

As presented in Figure 5(a), a good relationship between Na^+ and Cl^- was observed, implying the dissolution of halite. Moreover, plots above the 1:1 line suggest that excess of Na^+ may be derived from silicate weathering and/or cation exchange;

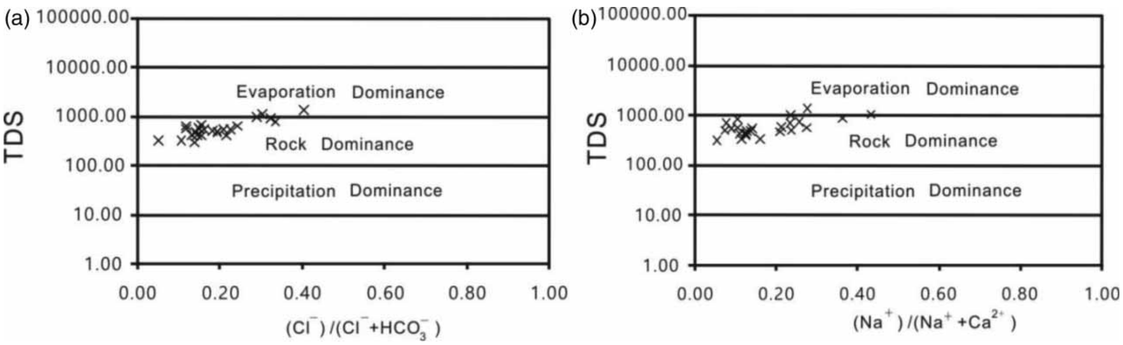

Figure 3 | Gibbs diagram of the groundwater samples.

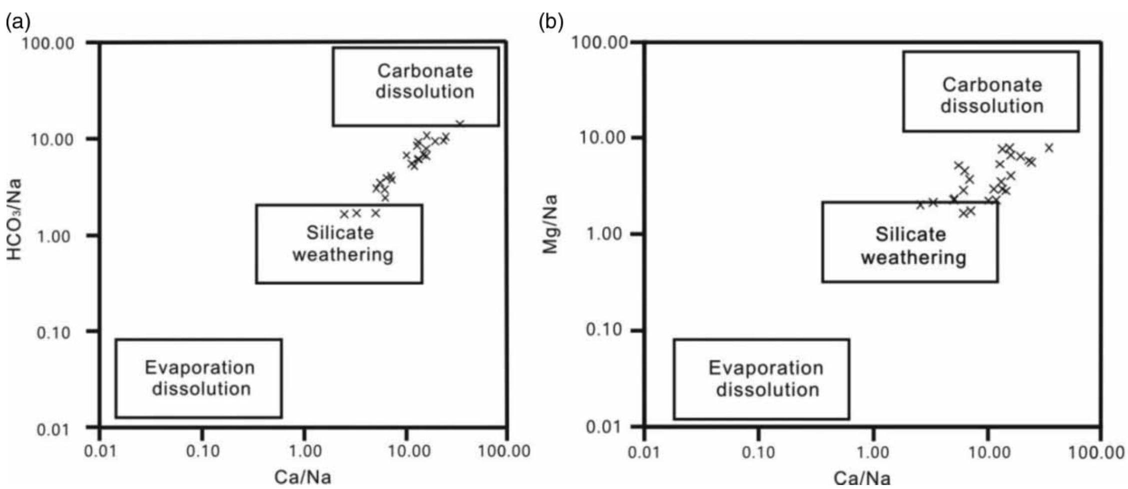

Figure 4 | Plots of Ca^{2+}/Na^+, HCO_3^-/Na^+ and Mg^{2+}/Na^+ of the groundwater samples.

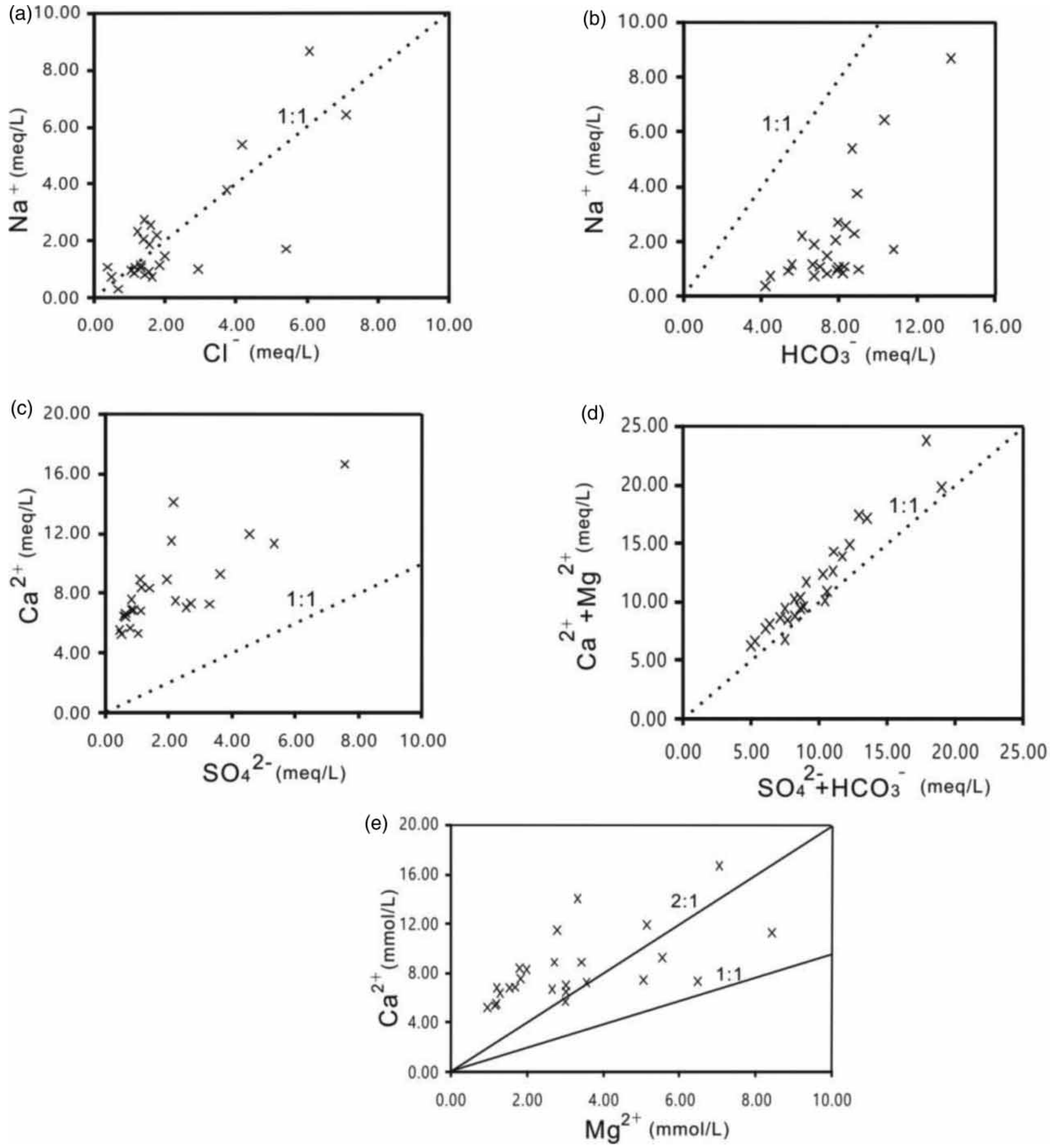

Figure 5 | Bivariate plots (a) [Na^+] versus [Cl^-], (b) [Na^+] versus [HCO_3^-], (c) [Ca^{2+}] versus [SO_4^-], and (d) [$Ca^{2+} + Mg^{2+}$] versus [$SO_4^{2-} + HCO_3^-$].

plots below the 1:1 line confirm that the groundwater hydrochemistry is affected by reverse cation exchange and/or agricultural activities. In Figure 5(b), the ratios of Na^+/HCO_3^- were concentrated on the right of the 1:1 line, suggesting that excess HCO_3- is mainly derived from silicate weathering (Chen *et al.* 2021). As can be seen in Figure 5(c), the ratios of Ca^{2+}/SO_4^{2-} exceeding 1 suggest that, in addition to dissolution of sulfate, the groundwater was also affected by silicate weathering. Thus, excess of Na^+ in Figure 5(a), excess of HCO_3^- in Figure 5(b) and excess of Ca^{2+} in Figure 5(c) together explain the silicate weathering such as soda feldspar and anorthite.

The relationship of ($Ca^{2+} + Mg^{2+}$) and ($SO_4^{2-} + HCO_3^-$) was employed to reveal the dissolution of sulfate, the weathering of silicate, the dissolution of carbonate and the cation exchange. Based on Figure 5(d), the samples scattered along the 1:1 line indicated that the groundwater composition is influenced by the dissolution of carbonate and sulfate. Moreover, the Ca^{2+}/Mg^{2+} molar ratio can further confirm dolomite dissolution, calcite dissolution, and silicate weathering. $Ca^{2+}/Mg^{2+} = 1$ implies the dissolution of dolomite, $1 < Ca^{2+}/Mg^{2+} < 2$ signifies the dissolution of calcite, and $Ca^{2+}/Mg^{2+} > 2$ indicates the weathering of silicate. In Figure 5(e), most samples were plotted in the areas of 1 ~ 2 and >2 (Pual *et al.* 2019). These results indicate that the calcium, magnesium and bicarbonate of the groundwater are primarily derived from the dissolution of carbonate and the weathering of silicate.

Principal component analysis (PCA) provides the most significant principal components with minimum loss of original information (Zhang *et al.* 2020). In this study, PCA with varimax rotation and Eigenvalues >1 were applied. As shown in Table 2, two principal components explained 86.61% of the total variance for the data. PC1, accounting for 68.78% of the total variance, exhibited strong positive loading of Na^+, Mg^{2+}, Ca^{2+}, Cl^-, SO_4^{2-}, and HCO_3^-. This factor represented the natural hydrochemical processes, including halite dissolution, sulfate dissolution, carbonate dissolution, and silicate weathering. PC2, occupying 17.83% of the total variance, has strong positive loading of K^+. This factor may be related to agricultural activities, such as use of potash fertilizer and pesticides.

The relationship between the hydrochemical parameters can be evaluated on the basis of the Pearson correlation matrix (Chotpantarat & Thamrongsrisakul 2021). As shown in Table 3, Cl^- exhibited a strong relationship with Na^+, Ca^{2+} and Mg^{2+}, indicating that the dissolution of chloride minerals is an important process for hydrochemical components. In addition, SO_4^{2-} was associated with Na^+, Ca^{2+} and Mg^{2+}, implying that they possibly derived from sulphate minerals. Moreover, the good relationship between HCO_3^- and Na^+, Ca^{2+} and Mg^{2+} can be used to explain the fact that these ions can be released from the weathering of silicate minerals and the dissolution of carbonate minerals.

Irrigation water quality assessment

According to the classification of EC value by the FAO, three classes were categorized to assess the salinity hazard (Mokoena *et al.* 2020). EC values of <750 μS/cm, 750 μS/cm-3,000 μS/cm, and >3,000 μS/cm were considered as no problem, an increasing problem, and a severe problem, respectively. As shown in Table 4, three samples are within the no problem

Table 2 | Principal component analysis of the groundwater samples

Species	PC1	PC2
Na^+	0.91	0.16
K^+	0.25	0.93
Mg^{2+}	0.91	0.14
Ca^{2+}	0.84	−0.38
Cl^-	0.92	−0.27
SO_4^{2-}	0.94	0.01
HCO_3^-	0.89	0.07
Eigen value	4.82	1.25
% of variance explained	68.78	17.83
% of cumulative variance	68.78	86.61

Table 3 | Correlation analysis of the groundwater samples

	Na^+	K^+	Mg^{2+}	Ca^{2+}	Cl^-	SO_4^{2-}	HCO_3^-
Na^+	1.00						
K^+	0.31	1.00					
Mg^{2+}	0.85**	0.26	1.00				
Ca^{2+}	0.60**	−0.04	0.61**	1.00			
Cl^-	0.81**	0.02	0.72**	0.91**	1.00		
SO_4^{2-}	0.87**	0.23	0.88**	0.79**	0.83**	1.00	
HCO_3^-	0.74**	0.28	0.83**	0.73**	0.78**	0.71**	1.00

**Correlation is significant at the 0.01 level (2-tailed).

Table 4 | Irrigation water quality classification based on various indices

Parameters	Range	Water type	No. samples	% samples
EC (Wilcox)	< 250	Excellent	0	0
	250–750	Good	3	12
	750–2,250	Permissible	22	88
	2,250–5,000	Doubtful	0	0
	> 5,000	Unsuitable	0	0
EC (FAO)	< 750	No problem	3	12
	750–3,000	Increasing problem	22	88
	> 3,000	Severe problem	0	0
SAR	0–10	Excellent	25	100
	10–18	Good	0	0
	18–26	Fair	0	0
	> 26	Poor	0	0
RSC	< 1.25	Safe	25	100
	> 1.25	Unsuitable	0	0
%Na	0–20	Excellent	20	80
	20–40	Good	5	20
	40–60	Permissible	0	0
	60–80	Doubtful	0	0
	> 80	Unsuitable	0	0

class, while the remaining twenty-two samples are classified as an increasing problem. Meanwhile, based on grading standards suggested by Wilcox (Ghazaryan *et al.* 2020), 88% of the water samples have a high EC value (750–2,250 μS/cm), which is permissible for irrigation. Only 12% of the samples with a value less than 750 μS/cm are found good for irrigation.

SAR is used to appraise the risk of sodicity of irrigation water. A high SAR can bring about a decrease in the permeability of the soil and result in compact and impervious soil (Zouahri *et al.* 2015; Ganiyu *et al.* 2018). In the present study, the calculated SAR values range between 0.17 and 2.75 meq/L. All of the samples are less than 10 meq/L, thus considered excellent for irrigation purpose.

RSC has also been employed to assess irrigation suitability. RSC values less than 1.25 meq/L and more than 1.25 meq/L are classified as safe and unsuitable for irrigation, respectively. In the study area, the calculated RSC values range from −13.31 to 0.45 meq/L with a mean value of −3.63 meq/L, which indicates that all the groundwater samples were considered safe for irrigation.

Percentage sodium (%Na), affecting plant growth, is used to appraise the effect on soil permeability and structure. %Na of the groundwater samples varies from 4.65 to 31.02, with a mean value of 13.91. Of the samples, 80% and 20% are excellent and good for irrigation, respectively. This indicates that the groundwater can be utilized for irrigation without any hazard.

The suitability of groundwater irrigation can be evaluated by USSL and Wilcox diagrams. According to the USSL diagram (Figure 6), 12% of groundwater samples fall in the category of C2S1, indicating medium salinity and low sodium hazard, which is good for irrigation. About 88% of the samples fall within the category of C3S1, suggesting the groundwater has a high salinity and low sodium hazard. This water can be used for salt-tolerant crops under favourable drainage conditions (Tiwari *et al.* 2017). As can be seen in the Wilcox diagram (Figure 7) (Sharma *et al.* 2017; Adimalla *et al.* 2018; Mebarki *et al.* 2021), the groundwater samples can been classified into two categories, viz., 88% belong to 'Good to Permissible', and 12% belong to 'Excellent to Good'.

Overall, the irrigation water quality of the study region is in a relatively appropriate condition. Nevertheless, rural issues with population decline, labor shortages, culture decline and ecological environment degradation have swept through developing and developed countries. In China, to address this situation of rural development, rural revitalization strategies and urban-rural integration with a series of policies aiming to promote rural development have been proposed and conducted to meet the demands of industrial prosperity, ecological livability, rural living conditions, effective governance, and prosperous life (Liu *et al.* 2020). As one important component of rural revitalization, groundwater has played a vital role in ecological environment construction. Solving the contradiction between supply and demand of water resources, and protecting the

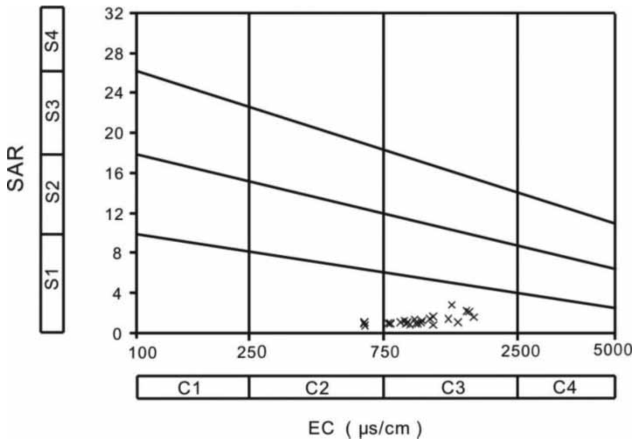

Figure 6 | USSL diagram for irrigation assessment.

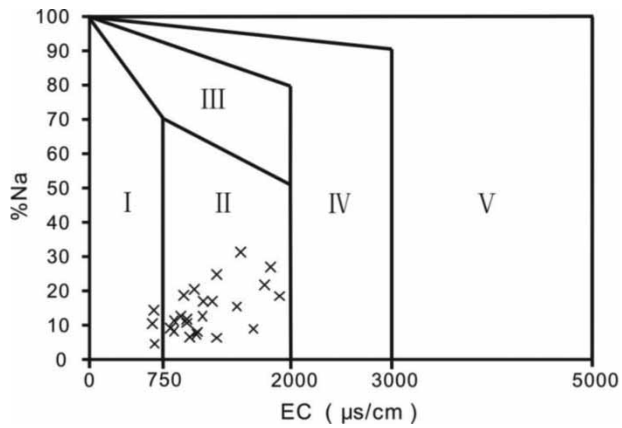

Figure 7 | Wilcox diagram for irrigation assessment I: Excellent to Good; II: Good to Permissible; III: Permissible to Doubtful, IV: Doubtful to Unsuitable, and V: Unsuitable.

freshwater ecosystem are the controlling factors for efficient management and utilization of water resources. So, identification of groundwater geochemistry and monitoring of groundwater quality are very meaningful for high-standard water quality management, water environment protection, and water resource utilization. Moreover, because of long-term use of groundwater as a water supply source, the decline of the groundwater table and the fluctuation of water quality have begun to occur. In recent years, some new water resource utilization and protection policies and methods have been introduced. For example, rainwater, and unpolluted and abundant river water have been considered as the standby water source to relieve the over-exploitation pressure of groundwater; central water supply and water quality monitoring have been conducted for sustainable ecological protection. These initiatives concerning water resource utilization and management need the most fundamental hydrochemical information. So, as one of the traditional agricultural production bases using groundwater, the study of hydrochemical characteristics and irrigation water quality of the groundwater aquifer in the Lan-gan region is essential to understand the groundwater geochemistry and its suitability for irrigation purposes. In addition, to achieve the goal of rural revitalization, long-term groundwater quality monitoring should be implemented by different groups, such as the supervision authorities, administrative departments, local residents, and scientific research departments.

CONCLUSIONS

In the present study, the hydrochemical characteristics and the suitability of irrigation were evaluated via Gibbs and Piper diagrams, ionic ratios, and multivariate statistical analysis. The following conclusions were drawn:

1. The order based on average concentration of cations and anions is $Ca^{2+} > Na^{+} > Mg^{2+} > K^{+}$ and $HCO_3^- > SO_4^{2-} > Cl^-$ respectively. Ca^{2+} and HCO_3^- are the most abundant cations and anions in the groundwater, respectively. The hydrochemical type is Ca-HCO_3 type.
2. Traditional graphical methods including Gibbs diagram and ionic ratios plots, and multivariate statistical analysis jointly explain the controlling hydrochemical processes. The ions mainly originate from halite dissolution, sulfate dissolution, carbonate dissolution, silicate weathering. In addition, excess of K^{+} may be derived from agricultural activities, such as the use of potash fertilizer and pesticides.
3. Based on the calculated results of %Na, SAR, EC and RSC, the groundwater can be utilized for irrigation without any hazard. According to the USSL diagram, 12% of groundwater samples fall in the category of C2S1, indicating medium salinity and low sodium hazard; 88% of the samples fall within the category of C3S1, suggesting the groundwater has high salinity and low sodium hazard. The Wilcox diagram shows that 88% of the samples belong to 'Good to Permissible', and 12% belong to 'Excellent to Good'.
4. As one important component of rural revitalization, groundwater has played a vital role in the ecological environment construction, solving the contradiction between supply and demand of water resources and protecting freshwater ecosystem, which are the controlling factors for efficient management and utilization of water resources. The study of hydrochemical characteristics and irrigation water quality of the groundwater aquifer in the Lan-gan region is essential to understand the groundwater geochemistry and its suitability for irrigation purposes.

ACKNOWLEDGEMENTS

This research was financially supported by the Excellent Top-notch Talents Cultivation Foundation of Colleges and Universities, Anhui Province, China (gxbjZD2020091 and gxgnfx2020106), the Natural Science Projects of Colleges and Universities, Anhui Province, China (KJ2020A0739), the Youth Project of Natural Science Foundation of Anhui Province (2008085QD175), and the Outstanding Academic and Technical Backbone of Suzhou University (2020XJGG11).

DATA AVAILABILITY STATEMENT

All relevant data are included in the paper or its Supplementary Information.

REFERENCES

Adimalla, N. 2020 Controlling factors and mechanism of groundwater quality variation in semiarid region of South India: an approach of water quality index (WQI) and health risk assessment (HRA). *Environ Geochem Health* **42**, 1725–1752.

Adimalla, N., Li, P. & Venkatayogi, S. 2018 Hydrogeochemical evaluation of groundwater quality for drinking and irrigation purposes and integrated interpretation with water quality index studies. *Environmental Process* **5**, 363–383.

Alemayehu, T., Leis, A. & Dietzel, M. 2020 Environmental isotope and hydrochemical characteristics of groundwater in central portion of Mekelle sedimentary outlier, northern Ethiopia. *Journal of African Earth Sciences* **171**, 103953.

Chen, K., Sun, L. & Xu, J. 2021 Statistical analyses of groundwater chemistry in the Qingdong coalmine, northern Anhui province, China: implications for water–rock interaction and water source identification. *Applied Water Science* **11**, 50.

Chotpantarat, S. & Thamrongsrisakul, J. 2021 Natural and anthropogenic factors influencing hydrochemical characteristics and heavy metals in groundwater surrounding a gold mine, Thailand. *Journal of Asian Earth Sciences.* **211**, 104692.

Ganiyu, S. A., Badmus, B. S., Olurin, O. T. & Ojekunle, Z. O. 2018 Evaluation of seasonal variation of water quality using multivariate statistical analysis and irrigation parameter indices in Ajakanga area, Ibadan, Nigeria. *Applied Water Science* **8**, 35.

Ghalib, H. B. 2017 Groundwater chemistry evaluation for drinking and irrigation utilities in east Wasit province, Central Iraq. *Applied Water Science* **7**, 3447–3467.

Ghazaryan, K., Movsesyan, H., Gevorgyan, A., Minkina, T., Sushkova, S., Rajput, V. & Mandzhieva, S. 2020 Comparative hydrochemical assessment of groundwater quality from different aquifers for irrigation purposes using IWQI: a case-study from Masis province in Armenia. *Groundwater for Sustainable Development* **11**, 100459.

Kshetrimayum, K. S. & Laishram, P. 2020 Assessment of surface water and groundwater interaction using hydrogeology, hydrochemical and isotopic constituents in the Imphal river basin, Northeast India. *Groundwater for Sustainable Development* **11**, 100391.

Li, Z., Li, Z., Song, L., Ma, J. & Song, Y. 2018 Environment significance and hydrochemical characteristics of supra-permafrost water in the source region of the Yangtze River. *Science of the Total Environment* **644**, 1141–1151.

Liu, Y., Zang, Y. & Yang, Y. 2020 China's rural revitalization and development: theory, technology and management. *Journal of Geographical Sciences* **30** (12), 1923–1942.

Ma, J., Sun, L., Chen, S., Gui, H. & Zhang, H. 2017 Geochemical study of the groundwater from coal bearing Aquifer in Zhuxianzhuang Coal Mine, Northern Anhui Province, China. *Nature Environment and Pollution Technology* **16** (4), 1217–1222.

Mebarki, S., Kharroubi, B. & Kendouci, M. A. 2021 Physicochemical evolution and evaluation of groundwater quality in Mougheul area (Southwest of Algeria). *Applied Water Science* **11**, 40.

Mokoena, P., Kanyerere, T. & Donker, J. V. B. 2020 Hydrogeochemical characteristics and evaluation of groundwater quality for domestic and irrigation purposes: a case study of the Heuningnes Catchment, Western Cape Province. South Africa. *SN Applied Sciences* **2** (9), 1–12.

Olea-Olea, S., Escolero, O., Mahlknecht, J., Ortega, L., Taran, Y., Moran-Zenteno, D. J., Zamora-Martinez, O. & Tadeo-Leon, J. 2020 Water-rock interaction and mixing processes of complex urban groundwater flow system subject to intensive exploitation: the case of Mexico City. *Journal of South American Earth Sciences* **103**, 102719.

Pazand, K., Khosravi, D., Ghaderi, M. R. & Rezvaniyanzadeh, M. R. 2018 Identification of the hydrogeochemical processes and assessment of groundwater in a semi-arid region using major ion chemistry: a case study of Ardestan basin in Central Iran. *Groundwater for Sustainable Development* **6**, 245–254.

Pual, R., Brindha, K., Gowrisankar, G., Tan, M. L. & Singh, M. K. 2019 Identifcation of hydrogeochemical processes controlling groundwater quality in Tripura, Northeast India using evaluation indices, GIS, and multivariate statistical methods. *Environmental Earth Sciences* **78**, 470.

Qian, J., Tong, Y., Ma, L., Zhao, W., Zhang, R. & He, X. 2018 Hydrochemical characteristics and groundwater source identification of a multiple aquifer system in a coal mine. *Mine Water and the Environment* **37**, 528–540.

Sharma, D. A., Rishi, M. S. & Keesari, T. 2017 Evaluation of groundwater quality and suitability for irrigation and drinking purposes in southwest Punjab, India using hydrochemical approach. *Applied Water Science* **7**, 3137–3150.

Sun, L. & Gui, H. 2015 Hydro-chemical evolution of groundwater and mixing between aquifers: a statistical approach based on major ions. *Applied Water Science* **5**, 97–104.

Tiwari, A. K., Ghione, R., Maio, M. D. & Lavy, M. 2017 Evaluation of hydrogeochemical processes and groundwater quality for suitability of drinking and irrigation purposes: a case study in the Aosta Valley region, Italy. *Arabian Journal of Geosciences* **10**, 264.

Xiao, J., Jin, Z. D., Wang, J. & Zhang, F. 2015 Hydrochemical characteristics, controlling factors and solute sources of groundwater within the Tarim River Basin in the extreme arid region, NW Tibetan Plateau. *Quaternary International* **380–381**, 237–246.

Yidana, S. M., Dzikunoo, E. A., Aliou, A. S., Adams, R. M., Chagbeleh, L. P. & Anani, C. 2020 The geological and hydrogeological framework of the Panabako, Kodjari, and Bimbilla formations of the Voltaian supergroup – Revelations from groundwater hydrochemical data. *Applied Geochemistry* **115**, 104533.

Zhang, H., Xu, g., Chen, X., Mabaire, A., Zhou, J., Zhang, Y., Zhang, G. & Zhu, L. 2020 Groundwater hydrogeochemical processes and the connectivity of multilayer aquifers in a coal mine with karst collapse columns. *Mine Water and the Environment* **39**, 356–368.

Zouahri, A., Dakak, H., Douaik, A., Khadir, M. E. & Moussadek, R. 2015 Evaluation of groundwater suitability for irrigation in the Skhirat region, Northwest of Morocco. *Environmental Monitoring and Assessment* **187**, 4184.

First received 24 March 2021; accepted in revised form 19 July 2021. Available online 30 July 2021